# Multiscaling to standard-scaling crossover in the Bray-Humayun model for phase-ordering kinetics

C. Castellano[1] and M. Zannetti[2]
[1]*Dipartimento di Scienze Fisiche, Università di Napoli, Mostra d'Oltremare, Padiglione 19, 80125 Napoli, Italy*
[2]*Istituto Nazionale di Fisica della Materia, Unità di Salerno and Dipartimento di Fisica, Università di Salerno, 84081 Baronissi (Salerno), Italy*

(Received 27 June 1995; revised manuscript received 25 September 1995)

The Bray-Humayun model for phase-ordering dynamics is solved numerically in one and two space dimensions with conserved and nonconserved order parameter. The scaling properties are analyzed in detail, and we find the crossover from multiscaling to standard scaling in the conserved case. Both in the nonconserved case, and in the conserved case when standard scaling holds an exponential tail in the scaling function is found.

PACS number(s): 64.60.Cn, 05.70.Fh, 64.60.My, 64.75.+g

## I. INTRODUCTION

In this paper we are concerned with scaling behavior in the phase-ordering dynamics of a system quenched below the critical point [1]. Specifically, we consider a system with an $N$-component order parameter $\vec{\phi}(\vec{x}) = (\phi_1(\vec{x}), ..., \phi_N(\vec{x}))$ quenched from high temperature to zero temperature whose dynamics are described by the zero noise Langevin equation

$$\frac{\partial \vec{\phi}(\vec{x},t)}{\partial t} = (i\vec{\nabla})^p \left[ \vec{\nabla}^2 \vec{\phi} - \frac{\partial V(\vec{\phi})}{\partial \vec{\phi}} \right], \tag{1}$$

where $p = 0$ for a nonconserved order parameter (NCOP), $p = 2$ for a conserved order parameter (COP), and $V(\vec{\phi}) = \frac{r}{2}\vec{\phi}^2 + \frac{g}{4}(\vec{\phi}^2)^2$ is the local potential with $(r < 0, g > 0)$. One of the reasons for the continuing interest in this type of problem is that a theoretical derivation of scaling on a first-principles basis is still lacking except for a few exactly soluble models [2,3].

Let us first give a qualitative description of what goes on during the phase-ordering process. Initially the system is prepared in a high-temperature state where the order parameter is spatially uncorrelated,

$$\langle \vec{\phi}(x,0) \cdot \vec{\phi}(x',0) \rangle = \Delta \delta_{\alpha\beta}(x - x'), \tag{2}$$

with $\alpha, \beta = 1, ..., N$ and $\Delta$ is a constant. The local order parameter probability distribution has a peak of width $\Delta$ centered about $\vec{\phi} = 0$. As the quench develops there is first a fast process (early stage) where this probability distribution, after a short time $t_0$, relaxes to equilibrium in the local potential, depleting the origin and developing a peak structure all around the bottom of the potential. In this span of time the local variance $\langle \vec{\phi}^2(\vec{x}, t_0) \rangle = S(t_0)$ loses memory of the initial condition $\Delta$ reaching a value very close to the final saturation value $S_{eq} = -r/g$. At this point the system is almost at equilibrium, namely ordered, on a short length scale. The subsequent time evolution amounts to coarsening of the ordered regions in order to reduce the excess interfacial free energy. During this process (late stage) the only important time dependence is in the linear size of the ordered regions, which typically grows according to a power law $L(t) \sim t^{1/z}$ with $z = 2$ for NCOP and $z = 3$ or $z = 4$ for COP, respectively, with $N = 1$ or $N > 1$. When $L(t)$ is large enough to dominate all other lengths the quantities of interest exhibit scaling. The main observables are the equal time order parameter correlation function $G(\vec{r}, t) = \langle \vec{\phi}(\vec{x}, t) \cdot \vec{\phi}(\vec{x} + \vec{r}, t) \rangle$ and the structure factor $C(\vec{k}, t)$ obtained by Fourier transforming $G(\vec{r}, t)$ with respect to space. The local variance of the order parameter is related to these quantities by $S(t) = G(\vec{r} = 0, t) = \int \frac{d\vec{k}}{(2\pi)^d} C(\vec{k}, t)$. Actually, we will be interested in the quantity

$$R(t) = r + gS(t) = g[S(t) - S_{eq}], \tag{3}$$

which monitors how the saturation value of $S(t)$ is reached.

According to the scaling hypothesis, all time dependence can be expressed through $L(t)$. The dominant behaviors for large $L(t)$ are given by

$$R(t) = -\frac{b}{L^\theta(t)}, \tag{4}$$

with $\theta = 2$ for systems with vector order parameter [4] and

$$C(\vec{k}, t) = S_{eq} f(L(t), kL(t)), \tag{5}$$

where the function $f(L, kL)$ must go over to $\delta(k)$ in the limit $L \to \infty$ in order to reproduce the Bragg peak corresponding to the final ordered state. In other words, $f(L, kL)$ is a smoothed out $\delta$ function on the scale $L(t)$ with the normalization property

$$\int \frac{d\vec{k}}{(2\pi)^d} f(L(t), kL(t)) = 1. \tag{6}$$

Experiments, numerical simulations, and soluble models, with the exception of the exact solution of the large-$N$ model with COP [3], yield the following form of scaling:

$$f(L, kL) = L^d F(kL), \tag{7}$$

1063-651X/96/53(2)/1430(11)/$06.00  

which we refer to as standard scaling. By contrast, when the model with $N = \infty$ and COP is solved one finds that this pattern of scaling is not obeyed. In that case the system behaves differently since next to $L(t)$ there is another divergent length $k_m^{-1}(t) \sim L/(\ln L)^{1/4}$, where $k_m(t)$ is the peak wave vector of the structure factor. Consequently, there appears a logarithmic correction in (4),

$$R(t) = -\frac{b}{L^2(t)}(\ln L)^{1/2}, \tag{8}$$

and in place of (7) one has the qualitatively different form

$$f(L, k/k_m) \sim (L^2 k_m^{2-d})^{\psi(k/k_m)}, \tag{9}$$

with $\psi(x) = 1 - (x^2 - 1)^2$. This pattern of scaling is referred to as multiscaling.

It should be stressed that the above solution of the $N = \infty$ model is the only available analytical solution of a system with COP. Hence, due to the difficulty of discriminating between multiscaling and standard scaling on the basis of the usual data collapse analysis, one may reasonably ask the question whether multiscaling might in fact be a generic feature of all systems with COP. In other words, setting $x = kL$ and neglecting logarithmic differences between $L$ and $k_m^{-1}$, i.e., letting $L = u/k_m$ with $u$ constant, one can postulate the general scaling form

$$f(L, x) = [L(t)]^{\varphi(x)} F(x), \tag{10}$$

which contains (7) and (9) as particular cases, respectively, with $\varphi(x) \equiv d$ and $\varphi(x) = d\psi(x/u)$. It is then a matter of computation or experiment to extract the spectrum of exponents $\varphi(x)$ and to check whether it is flat as in standard scaling or it is genuinely dependent, implying multiscaling.

This kind of analysis has been carried out on the data for the structure factor obtained from the simulation [5–7] of systems with COP and with $N$ ranging from 1 to 4 in two and three dimensions. In all of these cases the observed behavior of $\varphi(x)$ is consistent with the flat spectrum characteristic of standard scaling. Furthermore, analytical work of Bray and Humayun [8] (BH) on a model with $N$ large but finite and $d > 1$ suggests that standard scaling holds for any finite $N$, while multiscaling is only a feature of the special case $N = \infty$. Actually, the picture that BH put forward is that there exists a crossover time $t^*$ which depends on $N$ and the initial condition $\Delta$ and such that multiscaling holds for $t < t^*$ while for $t > t^*$ standard scaling sets in. Therefore, different asymptotic behaviors are obtained according to the order of the limits $t \to \infty$ and $N \to \infty$, as it was conjectured very early on by Oono [9]. If the limit $t \to \infty$ is taken first, standard scaling is observed asymptotically for any value of $N$, as long as $N < \infty$. Conversely, if the limit $N \to \infty$ is taken first, then the crossover time $t^*$ diverges and the asymptotic behavior exhibits multiscaling since the regime of standard scaling can never be reached.

What is at stake in this question of standard scaling vs multiscaling is the nature of the symmetry underlying scaling behavior [5]. The results of the simulations could be regarded as nonconclusive, since one could well imagine a spectrum $\varphi(x)$ which is dependent on $N$ and which interpolates between the $N = \infty$ behavior and the standard scaling behavior as $N$ gets smaller and smaller. Then, for values of $N$ of order unity, such as in the simulations, it might be difficult to decide whether a $\varphi(x)$ with a weak dependence on $x$ is evidence for standard scaling or for multiscaling. Instead, the result of BH is clear cut and states that the symmetry underlying asymptotic dynamics leads to standard scaling for any finite $N$. This result is quite important from the point of view of theory since theoretical progress in this field so far has heavily relied on the use of very clever but uncontrolled approximations [10]. This is due to the difficulty of developing systematic and controlled approximation schemes. An exception is the $1/N$ expansion for systems with NCOP [11]. The result of BH eliminates the possibility of extending the $1/N$ expansion as a systematic expansion scheme to the conserved case.

For the relevance of this issue, in this paper we have made a detailed study of the crossover from multiscaling to standard scaling through a comparative analysis of the numerical solution of the BH model with NCOP and with COP. Our aim is to proceed to an unbiased analysis of the scaling properties in order to have a check on the BH picture without any *a priori* assumption on the type of scaling, and to analyze in detail the difference between the conserved and nonconserved cases. In this respect our work is quite different from that of Rojas and Bray [12]. These authors do perfom a numerical solution of the BH model *after* the standard scaling ansatz has been made, while we first solve for the structure factor and then we proceed to the scaling analysis on the basis of the uncommitted general form (10).

The paper is organized as follows: in Sec. II we present the model and we elaborate on the difference between standard scaling and multiscaling, introducing the observables best suited to distinguish one from the other. In Sec. III we illustrate the method of solution with a test of its validity made by comparing numerical data with the analytical solution in the $N = \infty$ case. In Sec. IV we present the results for finite $N$ in one and two dimensions and in Sec. V we make some concluding remarks.

## II. BH MODEL, STANDARD SCALING, AND MULTISCALING

By using the Gaussian auxiliary field method of Mazenko [13], BH have derived [8] from (1) a closed equation of motion for the equal time correlation function within the framework of the $1/N$ expansion. Retaining nonlinear terms up to first order in $1/N$ one has

$$\frac{\partial G(\vec{r}, t)}{\partial t} = 2(i\vec{\nabla})^p \left[\vec{\nabla}^2 G - R(t)\left(G + \frac{1}{N}G^3\right)\right], \tag{11}$$

where $R(t)$ is a function of time which must be determined by the equilibrium requirement

$$\lim_{t\to\infty} G(\vec{r} = \vec{0}, t) = S_{eq} = -r/g. \tag{12}$$

The corresponding equation of motion for the structure factor is obtained after Fourier transforming with respect to space variables

$$\frac{\partial C(\vec{k},t)}{\partial t} = -2k^p\left[k^2+R(t)\right]C(\vec{k},t) - 2\frac{k^p}{N}R(t)D(\vec{k},t), \tag{13}$$

where $D(\vec{k},t)$ is the Fourier transform of $G^3(\vec{r},t)$. Notice that in the limit $N \to \infty$ (13) reduces to the equation which has been studied in [3],

$$\frac{\partial C(\vec{k},t)}{\partial t} = -2k^p\left[k^2+R(t)\right]C(\vec{k},t). \tag{14}$$

In this latter case $R(t)$ is defined self-consistently by (3). We shall retain this definition of $R(t)$ also in the finite $N$ case since from (13) follows that in order to reach equilibrium $R(t)$ must vanish and with the definition (3) the condition $\lim_{t\to\infty} R(t) = 0$ is an implementation of the requirement (12).

Although (11) or (13) have been derived by a truncation procedure based on the $1/N$ expansion, the solution of the equation is not of first order in $1/N$ since it contains all orders in $1/N$. Actually, it is not possible to assess precisely what is the relationship of this solution with the systematic $1/N$ expansion performed on the basic equation of motion (1). Presumably, it is some kind of infinite partial resummation intertwined with the uncontrolled approximation inherent in the use of the Gaussian auxiliary field method of Mazenko [10,13]. Hence, (11) or (13) should be regarded as the definition of a model, the BH model, for phase-ordering dynamics with an $N$-component vectorial order parameter which in the $N \to \infty$ limit reproduces the usual large-$N$ limit of (1) for the dynamics of the structure factor.

In order to make the scaling analysis of the BH model, let us integrate formally (13) from some instant of time $t_0$ onward,

$$\begin{aligned} C(\vec{k},t) = {} & C(\vec{k},t_0)e^{-2\left[k^{2+p}(t-t_0)+k^p\{Q(t)-Q(t_0)\}\right]} \\ & -2\frac{k^p}{N}\int_{t_0}^{t} dt' R(t')e^{-2\left[k^{2+p}(t-t')+k^p\{Q(t)-Q(t')\}\right]} \\ & \times D(\vec{k},t'), \end{aligned} \tag{15}$$

where $Q(t) = \int_0^t dt' R(t')$. Choosing $t_0$ in the scaling region, according to the standard scaling hypothesis we have the asymptotic behaviors

$$C(\vec{k},t) = S_{eq}L^d(t)F(x), \tag{16}$$

$$R(t) = -bL^{-2}(t), \tag{17}$$

$$Q(t)-Q(t_0) = \begin{cases} -2b\ln[L(t)/L_0] & \text{for NCOP} \\ -2b[L^2(t)-L_0^2] & \text{for COP,} \end{cases} \tag{18}$$

with $x = kL(t)$, $L(t) = t^{1/(2+p)}$, $L_0 = L(t_0)$, and $b$ is a positive constant to be determined.

Let us first consider the case of NCOP. Performing the above ansatz on (15) we find

$$\begin{aligned} F(x) = {} & F(x_0)(x/x_0)^{4b-d}e^{-2(x^2-x_0^2)} \\ & +S_{eq}^2\frac{4b}{N}\int_{x_0}^{x}\frac{dx'}{x'}(x/x')^{4b-d}e^{-2(x^2-x'^2)}\mathcal{D}(x'), \end{aligned} \tag{19}$$

where $x_0 = kL_0$ and

$$\begin{aligned} \mathcal{D}(\vec{x}') = {} & \int \frac{d\vec{x}_1}{(2\pi)^d}\frac{d\vec{x}_2}{(2\pi)^d}F(\mid \vec{x}'-\vec{x}_1\mid) \\ & \times F(\mid \vec{x}_1-\vec{x}_2\mid)F(x_2). \end{aligned}$$

The condition (12) requires

$$\int \frac{d\vec{x}}{(2\pi)^d}F(x) = 1, \tag{20}$$

which gives an equation for $b$. Letting $x_0 \to 0$ and requiring (20) to be satisfied, in the $N = \infty$ case we obtain $4b - d = 0$ and

$$F(x) = F(0)e^{-2x^2}, \tag{21}$$

while for finite $N$ we find $4b - d < 0$.

Let us now go to the COP case. Making the scaling ansatz into (15) with $p = 2$ we find

$$\begin{aligned} F(x) = {} & F(x_0)(x_0/x)^d e^{-2[(x^4-x_0^4)-2b(x^2-x_0^2)]} \\ & +\frac{8bS_{eq}^2}{Nx^d}\int_{x_0}^{x}dx'x'^{d+1}e^{-2\left[(x^4-x'^4)-2b(x^2-x'^2)\right]}\mathcal{D}(x'). \end{aligned} \tag{22}$$

Now, if we let again $x_0 \to 0$, in the $N = \infty$ case $F(x)$ vanishes identically and it is not possible anymore to satisfy (20). This is the breakdown of standard scaling in the large-$N$ limit which leads to multiscaling [3]. Conversely, if $N$ is kept finite, (22) yields

$$F(x) = \frac{8bS_{eq}^2}{Nx^d}\int_0^x dx'x'^{d+1}e^{-2\left[(x^4-x'^4)-2b(x^2-x'^2)\right]}\mathcal{D}(x'). \tag{23}$$

This is the equation that BH have solved, finding a nontrivial solution and reaching the conclusion that for any finite $N$ standard scaling holds also for systems with COP.

According to the above discussion the first term in the right-hand side of (15), the one which survives after $N \to \infty$, is responsible for multiscaling behavior while the second one is responsible for standard scaling. The competition of these two terms is expected to generate a crossover time $t^*$ such that multiscaling behavior of the type found with $N = \infty$ holds for $t < t^*$ while standard scaling eventually sets in for $t > t^*$.

In the following we will make a numerical study of the scaling properties of the structure factor in the BH model on the basis of the general scaling form (10). The primary interest is in the discrimination between standard scaling and multiscaling and in the study of the crossover. The analysis will be carried out through the behavior of the spectrum of exponents $\varphi(x)$ as described in the Introduction and through the behavior of the quantity

$$Y(t) = -R(t)L^2(t), \tag{24}$$

which discriminates between standard scaling and multiscaling on the basis of the asymptotic behaviors

$$Y(t) \begin{cases} = b(N) & \text{for standard scaling} \\ \sim (\ln t)^{1/2} & \text{for multiscaling.} \end{cases} \tag{25}$$

## III. METHOD OF SOLUTION AND NUMERICAL RESULTS FOR $N = \infty$

In order to investigate the scaling properties of the BH model the discretized version of (11) is integrated numerically via a simple finite difference first-order Euler scheme. The initial condition is given by $G(\vec{r},0) = \Delta$ for $\vec{r} = 0$ and $G(\vec{r},0) = 0$ elsewhere. The boundary conditions are chosen to be periodic, but open conditions have been tested and found not to make a difference on the final results. From the values of $G(\vec{r},t)$ the structure factor is then obtained via a fast Fourier transform and from these two functions all quantities of interest are computed.

Two opposite requirements enter in the choice of the parameters of the numerical solution, and in particular of the linear dimension $L$ of the system. A large number of lattice sites is desirable to avoid that discretization of space may hide the subtle difference between standard scaling and multiscaling. On the other hand, fewer sites speed up the computation and investigation of later times is feasible. Resorting to parallel computing, we have managed to perform the numerical integration on large systems and for sufficiently long times. In principle, one can solve (13) to obtain directly the structure factor, but the presence in (13) of a double convolution integral, which cannot be parallelized efficiently, makes this alternative computational scheme much slower.

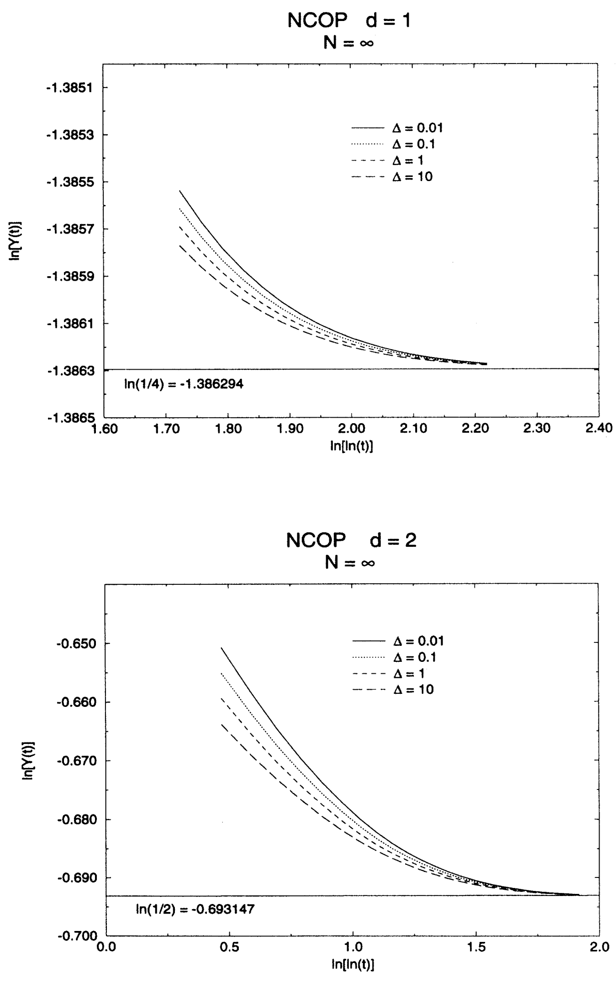


FIG. 1. $\ln Y(t)$ for NCOP with $N = \infty$ and different values of $\Delta$ displaying the approach to $\ln(1/4) = -1.386\,29$ for $d = 1$ and to $\ln(1/2) = -0.693\,14$ for $d = 2$ as predicted by (25).

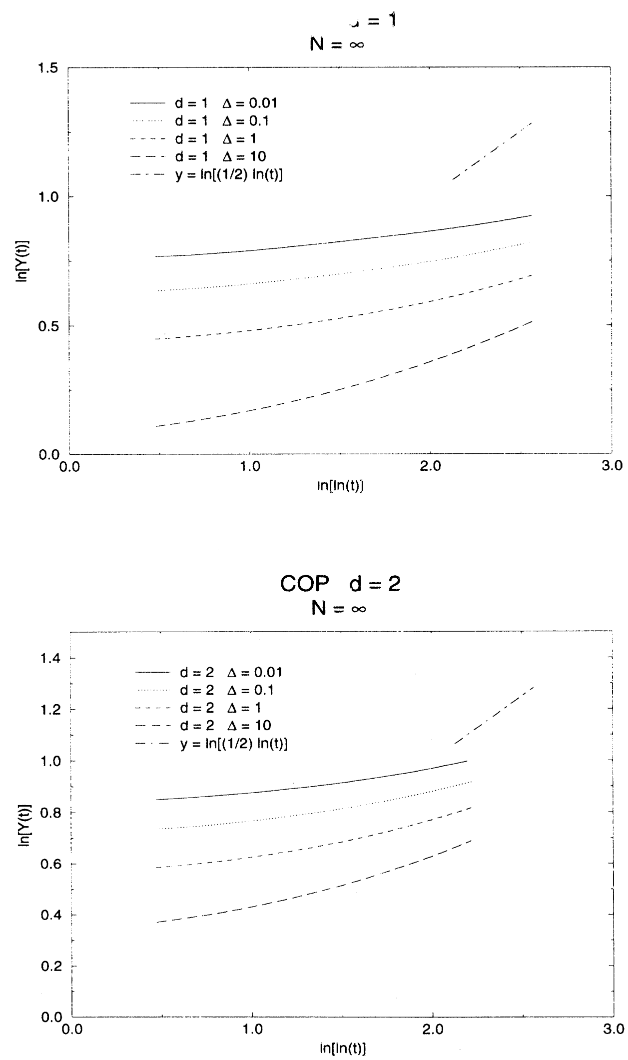


FIG. 2. $\ln Y(t)$ for COP with $N = \infty$ and different values of $\Delta$.

For all runs the value of the mesh size has been taken as $\Delta x = 1$, while the time step $\Delta t$ has been changed depending on the values of $N$ and $d$ in order to prevent numerical instabilities. In particular, for NCOP, $\Delta t = 0.01$ for all values of $d$ and $N$ except when $N = 10$. In this latter case, we have taken $\Delta t = 0.005$. For COP, $\Delta t = 0.05$ for $d = 1$ and $\Delta t = 0.01$ for $d = 2$. For the parameters of the potential $V(\vec{\phi})$ we have chosen the values $r = -10$ and $g = 1$.

After computing the structure factor $C(\vec{k}, t)$ for several different times, the spectrum of scaling exponents $\varphi(x)$ can be obtained by using the general scaling form (10), which can be rewritten as

$$\ln C(\vec{k}, t) = \varphi(x) \ln L(t) + \ln F(x), \tag{26}$$

where $L(t) = t^{\frac{1}{2+p}}$ and $x = kL(t)$. Hence, plotting $\ln C(x/L(t), t)$ vs $\ln L(t)$ at fixed $x$ one can measure $\varphi(x)$ from the slope and $F(x)$ from the intercept with the vertical axis. However, from the numerical point of view it is more convenient to use a slightly different procedure, because $x/L(t)$ could turn out to be too small or too big with respect to the available values of $k$. For the NCOP case, $C(\vec{k}, t)$ is computed not as $C(x/L(t), t)$ but as $C(xk_2(t), t)$, where $k_2(t)$ is defined by $C(k_2(t), t) = C(0, t)/2$. This introduces in Eq. (26) an additional constant term given by the logarithm of the proportionality factor between $L(t)$ and $k_2(t)$. Furthermore, the error in the determination of $k_2(t)$ and $C(xk_2(t), t)$ is greatly reduced by the use of linear interpolation between the discrete values of $k$. In the COP case $C(\vec{k}, t)$ is computed as $C(xk_m(t), t)$ where $k_m(t)$ is the peak wave vector of the structure factor. The logarithm of $C(xk_m(t), t)$ is plotted versus $\ln[L^2(t)k_m^{2-d}(t)]$. With this choice, for $N = \infty$, the slope $\varphi(x)$ is given by $d\psi(x)$ rather than by $d\psi(x/u)$. This makes the comparison between numerical and analytical results easier also for $N < \infty$. Again the quality of the fit is enhanced by determining the peak wave vector and $C(xk_m(t), t)$ via

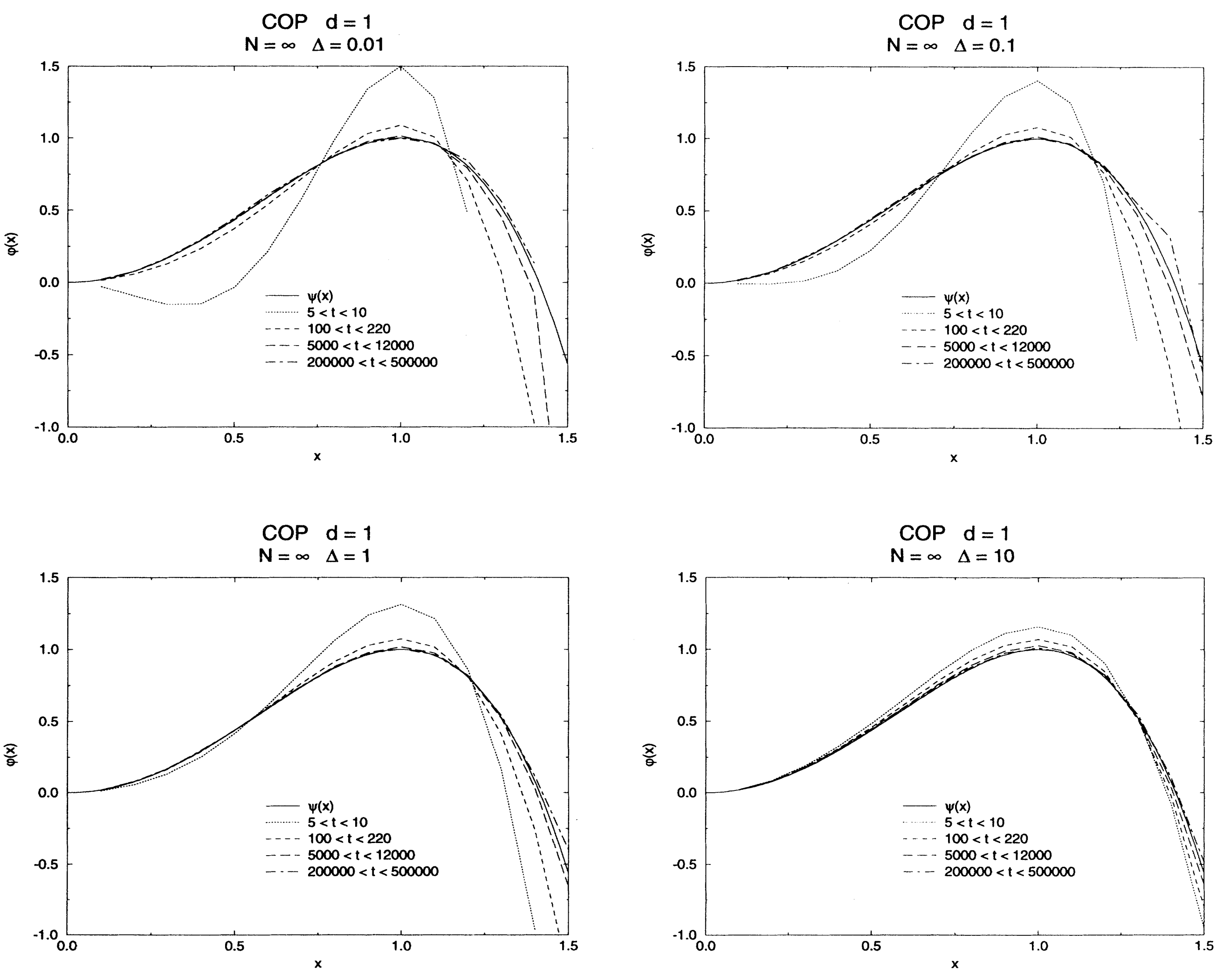


FIG. 3. Time evolution of $\varphi(x)$ for COP with $N = \infty$, $d = 1$, and different values of $\Delta$.

cubic and linear interpolation, respectively.

In order to check the quality of the numerical method, let us consider the $N = \infty$ case where exact analytical results are available. We solve for $C(\vec{k}, t)$ in one and two space dimensions with $\Delta$ ranging in the interval $(0.01, 10)$. We discuss first the case of NCOP and then the case with COP. The motivation for doing this computation is also to establish clearly the behavior of observables according to standard scaling (NCOP) and to multiscaling (COP).

### A. NCOP

In order to analyze the behavior of $Y(t)$ in Fig. 1 $\ln[Y(t)]$ has been plotted versus $\ln(\ln t)$ for $d = 1$ and $d = 2$. In both cases $\ln[Y(t)]$ displays the approach to the asymptotic constant value $\ln(d/4)$ of standard scaling predicted by (25) through a transient dependent on the initial condition $\Delta$. No detectable dependence on the initial condition is found in the behavior of $\varphi(x)$ which in agreement with (16) follows the constant behavior $\varphi(x) \equiv d$. Similarly, the numerical results for the scaling function reproduce accurately the Gaussian behavior (21).

### B. COP

With COP the behavior of $\ln[Y(t)]$ is qualitatively different from what we had above with NCOP. In place of the relaxation to a constant value now (Fig. 2) there is an upward increasing trend revealing multiscaling. In the time of the computation there is still a dependence on the initial condition $\Delta$, with a faster convergence to the asymptotic behavior $\sim \ln[1/2\ln(t)]$ given by (25) for

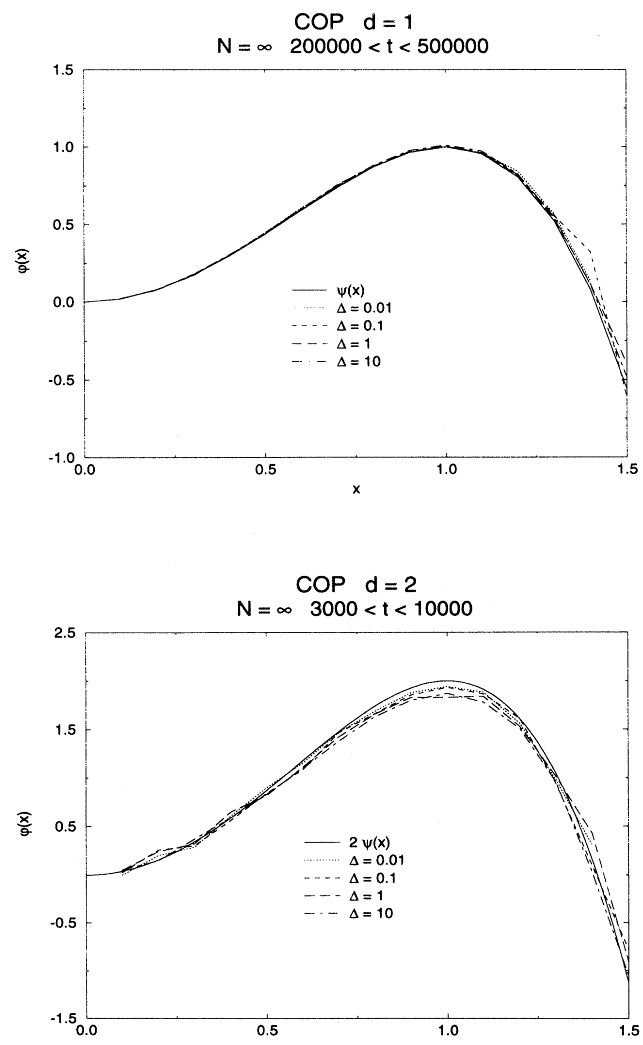


FIG. 4. Late stage $(200\,000 < t < 500\,000)$ multiscaling behavior of $\varphi(x)$ for COP with $N = \infty$, revealing independence from the initial condition.

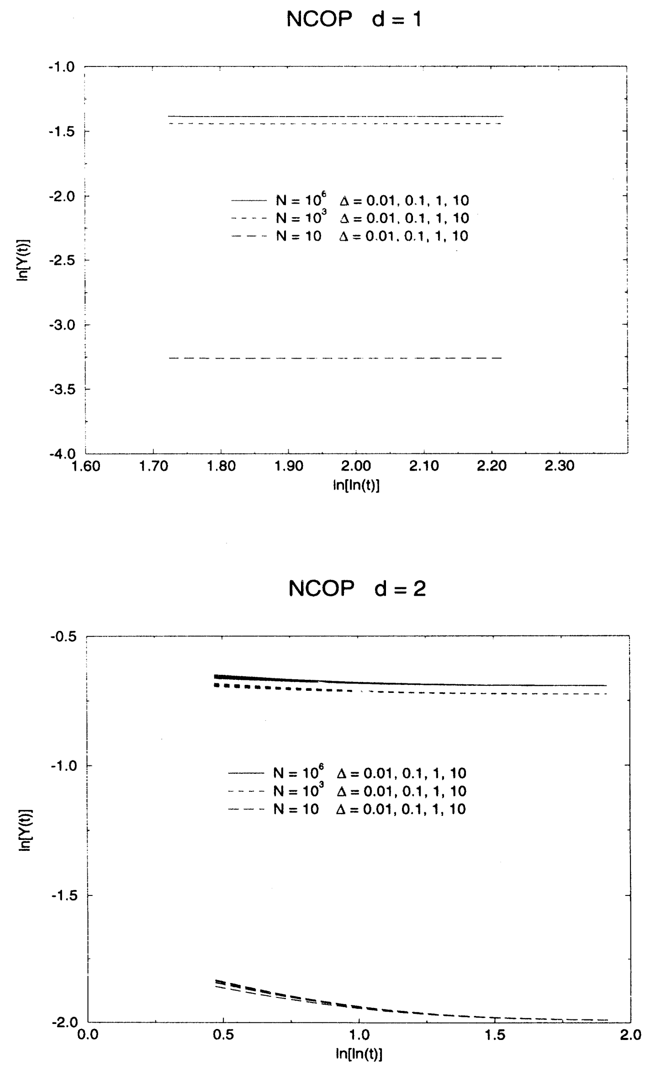


FIG. 5. $\ln Y(t)$ for NCOP with $N = 10, 10^3, 10^6$. The $\Delta$-dependent transient preceding the asymptotic behavior is negligible in this scale for $d = 1$.

higher values of $\Delta$. The asymptotic behavior has not been reached in the time of the computation due to the much slower dynamics of COP.

Multiscaling is most clearly illustrated by the behavior of $\varphi(x)$. It is interesting to see how the spectrum of exponents depends on the time interval of observation. In Fig. 3 the evolution of $\varphi(x)$ in subsequent time intervals has been plotted for different values of $\Delta$ and for $d = 1$. Results for $d = 2$ are similar. Figure 3 demonstrates the relaxation of $\varphi(x)$ to the asymptotic behavior given by $\varphi(x) = d\psi(x)$. As remarked above the relaxation is faster for higher values of $\Delta$. The late stage results are displayed in Fig. 4 both for $d = 1$ and $d = 2$, showing the independence from $\Delta$ of the computed $\varphi(x)$. This suggests that, at least in the range of $x$ considered, $\varphi(x)$ reaches the asymptotic regime faster than $Y(t)$.

## IV. RESULTS FOR FINITE $N$

In this section we illustrate the solution of the BH equation with finite $N$ obtained by the numerical method described in the preceding section.

### A. NCOP

The standard scaling behavior of systems with NCOP is manifested (Fig. 5) first of all in the behavior of $Y(t)$,

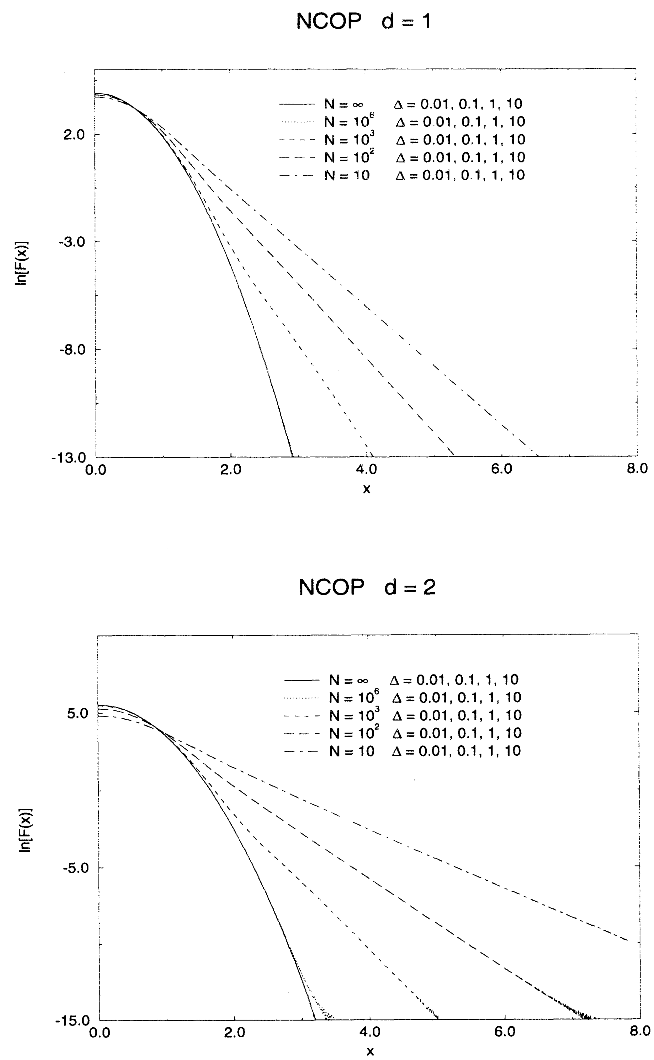


FIG. 6. Plot of the scaling function for NCOP demonstrating exponential decay in the tails.

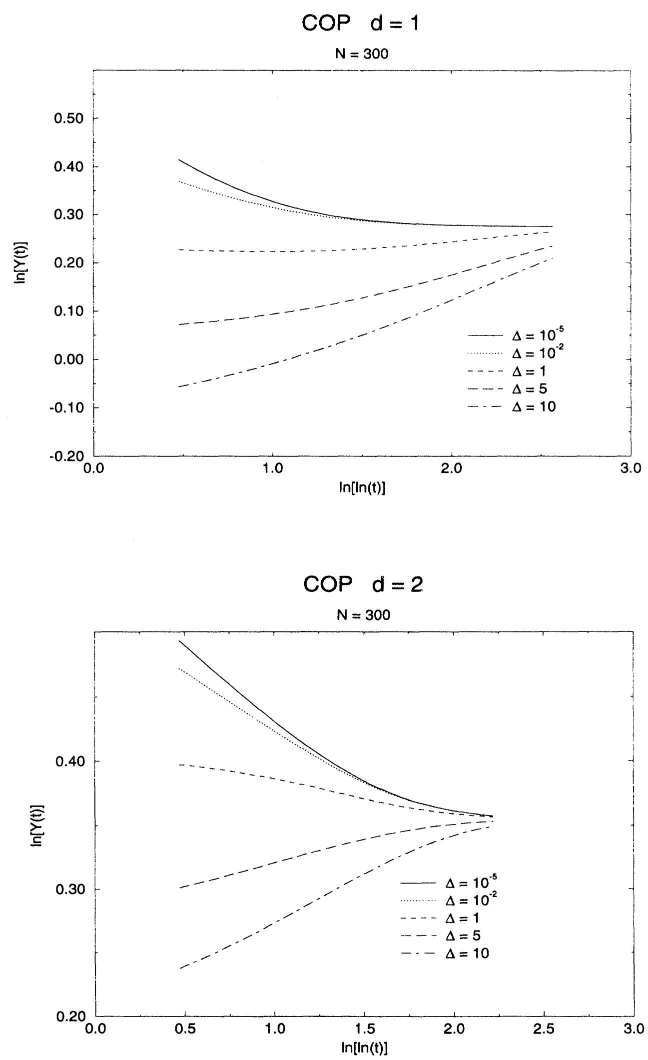


FIG. 7. $\ln Y(t)$ for COP with $N = 300$ displaying, in the preasymptotic regime, the switch from standard scaling to multiscaling with increasing $\Delta$.

which according to (25) goes to a constant asymptotic value $b(N)$ smaller than $d/4$ and decreasing monotonically with $N$. The transient preceding the asymptotic behavior now depends both on $\Delta$ and $N$. Asymptotic behavior independent of $\Delta$ and $N$ instead is manifested by $\varphi(x)$ which displays with great accuracy the flat behavior $\varphi(x) \equiv d$. A significant $N$ dependence shows up (Fig. 6), however, in the scaling function $F(x)$. According to the analysis of Sec. II, a deviation from Gaussian behavior is expected for finite $N$ in the tail of $F(x)$ due to the second term in the right hand side of (19) and this deviation clearly should be more important for small values of $N$. The plot of $\ln F(x)$ vs $x$ reveals the interesting feature that the tail decays exponentially rather than following the generalized Porod law $\sim x^{-(d+N)}$ [14]. Simulations of a system with NCOP and $N > d$ have been performed by Toyoki [15], finding a tail which decays with a power much higher than that of the generalized Porod law. Our result suggests that an exponential fit might be appropriate also in this case.

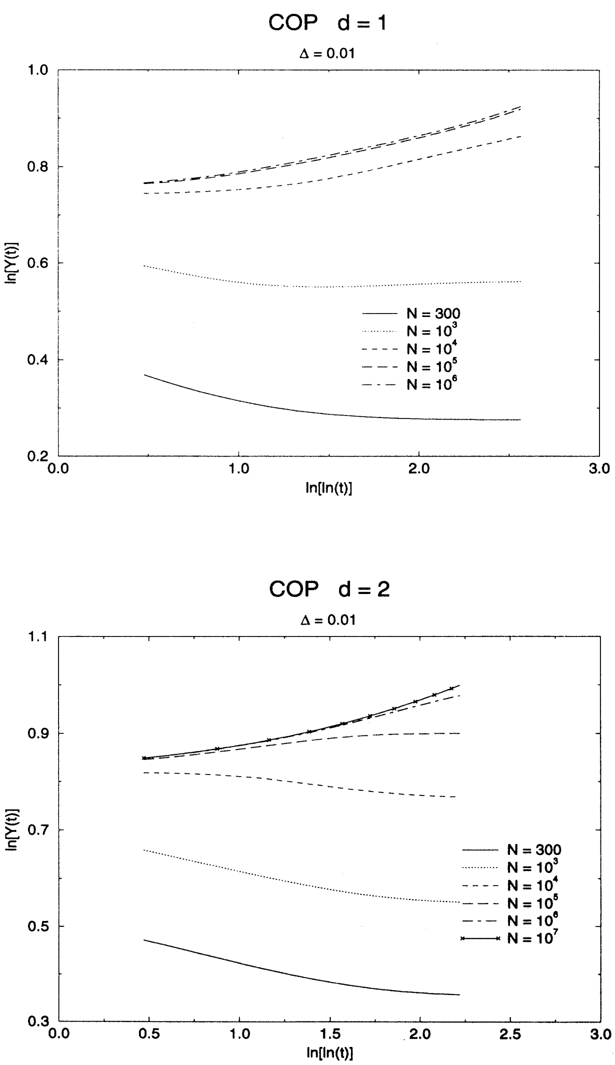


FIG. 8. $\ln Y(t)$ for COP with $\Delta = 0.01$ displaying, in the preasymptotic regime, the switch from standard scaling to multiscaling with increasing $N$.

## B. COP

The picture is more complex and interesting with COP. Figures 7 and 8 display, respectively, the behavior of $\ln[Y(t)]$ for a fixed value of $N$ with varying $\Delta$ and vice versa for a fixed value of $\Delta$ with varying $N$. What emerges from a comparison with the analogous data for $N = \infty$ is that for fixed $N$ (here $N = 300$) the behavior is of the standard scaling type for $\Delta$ sufficiently small (e.g., $\Delta = 10^{-5}$) while it is of the multiscaling type for $\Delta$ large ($\Delta = 10$), with an interpolating behavior for intermediate values of $\Delta$. Similarly, for $\Delta$ fixed ($\Delta = 0.01$) the behavior goes from standard scaling for $N = 300$ toward multiscaling as $N$ grows very large. This pattern fits with the crossover picture illustrated in the Introduction, allowing for a crossover time $t^*$ which grows both with $N$ and with $\Delta$. Standard scaling then applies when the values of $N$ and $\Delta$ are such that $t^*$ is very short. For higher values of $N$ and $\Delta$, instead, $t^*$ can be made large enough for the system to develop multiscaling behavior before the asymptotic standard scaling behavior is reached. If only multiscaling behavior is observed, as, for instance, for $N = 300$ and $\Delta = 10$ or for $N = 10^6$ and $\Delta = 0.01$, it means that for those values of $N$ and $\Delta$ the crossover time $t^*$ is larger than the maximum time reached in the numerical computation. From these data it is very difficult, though, to infer the quantitative dependence of $t^*$ on $N$ and $\Delta$. BH have proposed [8] the analytical form $t^* \sim (\Delta N)^{4/d}(\ln N)^3$, which holds for $d > 1$. However, the predictions from this formula seem to be quite off from what we observe. For instance, for $N = 300$, $\Delta = 1$, and $d = 2$ the above formula gives $t^* \sim 10^7$, which is large enough to expect an observable crossover, while for these values of the parameters we find only standard scaling behavior (Figs. 7 and 9).

As we have seen with $N = \infty$ the distinction between standard scaling and multiscaling is most effectively manifested through $\varphi(x)$. Thus, according to the crossover picture obtained from $Y(t)$, it should be possible to produce standard scaling or multiscaling in $\varphi(x)$ by properly choosing the values of $N$ and $\Delta$. In Fig. 9 we have analyzed the evolution of $\varphi(x)$ in time for $\Delta = 0.01$ and different values of $N$ for $d = 2$ (similar results are obtained for $d = 1$). For $N$ ranging from $10^2$ to $10^4$, $\varphi(x)$ displays standard scaling over all time intervals, implying that $t^*$ is of order 1. For larger values $N = 10^5, 10^6$ one can definitely recognize a multiscaling type of behavior over the initial time intervals, evolving toward standard scaling in the later time intervals. Here it is difficult to assess the value of $t^*$, but it must be of the order of magnitude of the time of observation. Finally, for $N = 10^7$ the behavior of $\varphi(x)$ is of the multiscaling type over all time intervals, implying that $t^*$ exceeds the maximum time reached in the numerical computation.

In order to complete the analysis in Fig. 10 we have plotted the logarithm of the scaling function $F(x)$ vs $x$ for different values of $N$, finding again an exponential tail as in the NCOP case. In this case there are small secondary peaks superimposed on the tail which scale like $L(t)$ and which become more pronounced as $N$ grows. Exponential tails have been observed previously in the simulation of systems with COP and without topological defects [7]. Finally, in agreement with Rojas and Bray [12], we find that the peak of $F(x)$ is well fitted by the quartic exponential form appearing in the BH analytical solution.

## V. CONCLUSIONS

The main motivation for this paper was to investigate in detail the onset of standard scaling in the BH model for phase-ordering kinetics with COP and finite $N$. We have done this by a comparative study of the numerical solution of the model with NCOP and with COP. In both cases eventually there is standard scaling, but the difference is much more profound than just the value of the growth exponent ($z = 2$ for NCOP and $z = 4$ for COP) when the whole development of the dynamics is taken into account. As probes for scaling we have used $Y(t)$ and $\varphi(x)$. Parameters of the quench are the initial condition $\Delta$ and the number of components $N$ of the order parameter.

The picture for NCOP is the following. Starting from a uniform initial condition $C(\vec{k}, t = 0) = \Delta$, after a short transient of duration $t_0$ during which information on the initial condition is lost, the dynamics of standard scaling sets in, with ordered regions growing like $L(t) \sim t^{1/2}$, $\varphi(x) \equiv d$, and the scaling form (16) obeyed. The only place where there remains a detectable transient dependence on the initial condition $\Delta$ for longer times than $t_0$ is in the behavior of $Y(t)$, which displays a very slow approach to the constant asymptotic behavior. This means

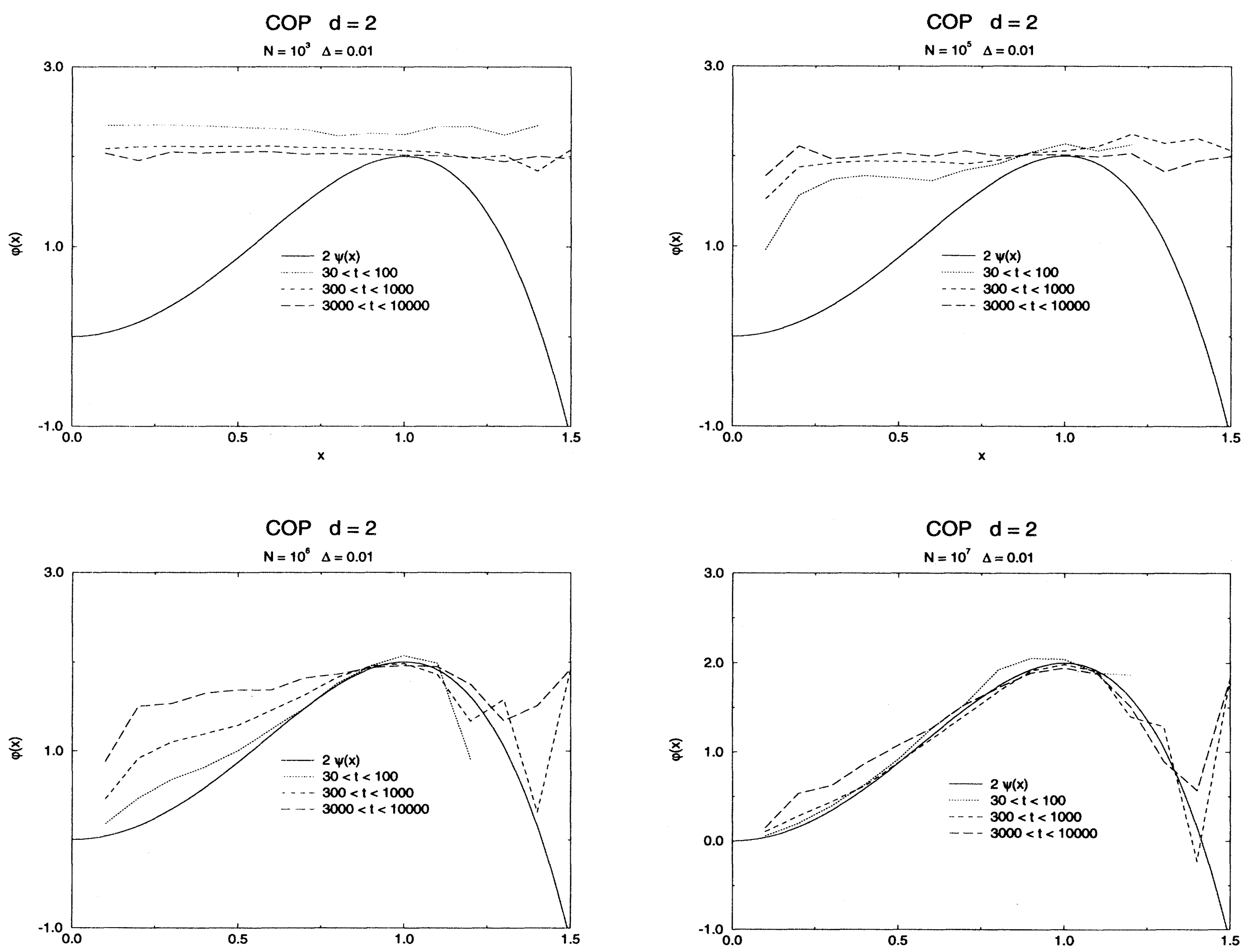


FIG. 9. Time evolution of $\varphi(x)$ for COP with $\Delta = 0.01$, $d = 2$, and different values of $N$.

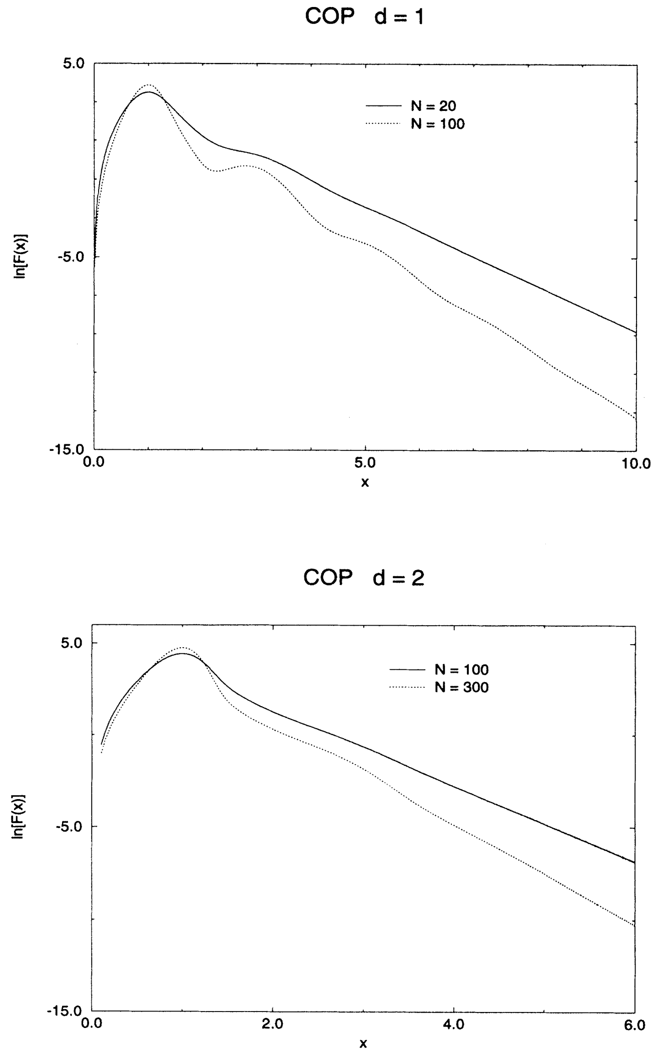


FIG. 10. Plot of the scaling function for COP demonstrating exponential decay in the tails. Computations have been carried out with $\Delta = 0.01$.

that in the scaling ansatz for $R(t)$ there is a slow correction with a small amplitude. This pattern of behavior for NCOP is the same for any value of $N$, including $N = \infty$.

By contrast, with COP the way the system eventually reaches standard scaling is more complicated and depends on $N$ due to the existence of the two characteristic times $t_0$ and $t^*$. Only if $t^* \sim t_0$ is there no observable difference between COP and NCOP. Instead, if $t^*$ is sufficiently larger than $t_0$ the system displays multiscaling in between $t_0$ and $t^*$, before the standard scaling regime is reached. In this sense multiscaling is not only a feature of the special case $N = \infty$, but is relevant also for systems with finite $N$. The existence of a connection between multiscaling and standard scaling is expected after recognizing that these are the two asymptotic features of a crossover process. More specifically, let us consider a general scaling form containing both regimes

$$C(\vec{k}, t, N) = L^{d\psi(x)} \mathcal{F}\left(x, \frac{N}{L^a}\right), \tag{27}$$

with $x = k/k_m$, $a$ an index to be determined, and $\mathcal{F}$ a function with the limiting behaviors

$$\mathcal{F}\left(x, \frac{N}{L^a}\right) = \begin{cases} 1 & \text{if } N/L^a \gg 1 \\ A(\frac{N}{L^a})^{\alpha(x)} & \text{if } N/L^a \ll 1, \end{cases} \tag{28}$$

where $A$ and $\alpha(x)$ also must be determined. The above form clearly yields multiscaling if the limit $N \to \infty$ is taken. If instead $N$ is kept finite and $L(t)$ becomes large one has

$$C(\vec{k}, t, N) = AL^{d\psi(x) - a\alpha(x)} N^{\alpha(x)} \tag{29}$$

and imposing $d\psi(x) - a\alpha(x) = d$ one finds standard scaling,

$$C(\vec{k}, t, N) = AL^d e^{-\frac{d}{a}[1-\psi(x)] \ln N} = AL^d e^{-\frac{d}{a}(x^2-1)^2 \ln N}, \tag{30}$$

exactly with the BH scaling function, revealing the deep connection between multiscaling and standard scaling as the multiscaling spectrum $\psi(x)$ dictates the form of the scaling function in the standard-scaling regime. This multiscaling to standard-scaling crossover in principle could be observed also in systems with realistic values of $N$ by making $t^*$ large enough exploiting the dependence of $t^*$ on $\Delta$. In this respect it might be interesting to check this hypothesis on the simulations of Refs. [5–7] performed with values of $\Delta$ making $t^*$ sufficiently large.

Finally, the finding of exponential tails in the scaling functions is quite interesting and simulations on cell dynamical systems are under way in order to check on the existence of these tails in systems with $N > d + 1$.

## ACKNOWLEDGMENTS

It is a pleasure to thank Antonio Coniglio and Sharon Glotzer for the many clarifying and quite instructive discussions on the subject of this work. We also wish to thank A. Bray for suggestions that have led to an improvement of the paper. One of us (C.C.) wishes to thank the Polymers Division of the National Institute of Standards and Technology for hospitality during completion of this work and the Boston University Center for Computational Science for generous use of their computing facilities.

[1] For a recent review see A.J. Bray, Adv. Phys. **43**, 357 (1994).

[2] G.F. Mazenko and M. Zannetti, Phys. Rev. Lett. **53**, 2106 (1984); A.J. Bray, J. Phys. A **22**, L67 (1990); J.G. Amar and F. Family, Phys. Rev. A **41**, 3258 (1990); T.J. Newman, A.J. Bray, and M.A. Moore, Phys. Rev. B **42**, 4514 (1990).

[3] A. Coniglio and M. Zannetti, Europhys. Lett. **10**, 575

(1989).
[4] F. Liu and G.F. Mazenko, Phys. Rev. B **45**, 6989 (1992).
[5] A. Coniglio, Y. Oono, A. Shinozaki, and M. Zannetti, Europhys. Lett. **18**, 59 (1992).
[6] M. Mondello and N. Goldenfeld, Phys. Rev. E **47**, 2384 (1993); M. Siegert and M. Rao, Phys. Rev. Lett. **70**, 1956 (1993).
[7] M. Rao and A. Chakrabarti, Phys. Rev. E **49**, 3727 (1994).
[8] A.J. Bray and K. Humayun, Phys. Rev. Lett. **68**, 1559 (1992).
[9] Y. Oono (private communication).
[10] C. Yeung, Y. Oono, and A. Shinozaki, Phys. Rev. E **49**, 2693 (1994); S. De Siena and M. Zannetti, *ibid.* **50**, 2621 (1994).
[11] T.J. Newman and A.J. Bray, J. Phys. A **23**, 4491 (1990).
[12] F. Rojas and A.J. Bray, Phys. Rev. E **51**, 188 (1995).
[13] G.F. Mazenko, Phys. Rev. Lett. **63**, 1605 (1989); Phys. Rev. B **42**, 4487 (1990); **43**, 5747 (1991).
[14] A.J. Bray and S. Puri, Phys. Rev. Lett. **67**, J670 (1991); H. Toyoki, Phys. Rev. B **45**, 1965 (1992).
[15] H. Toyoki, Mod. Phys. Lett. B **7**, 397 (1993).